ELSEVIER

Journal of Alloys and Compounds 344 (2002) 207–211

Journal of ALLOYS AND COMPOUNDS

www.elsevier.com/locate/jallcom

Characterization of erbium oxide sol–gel films and devices by grazing incidence X-ray reflectivity

S.L. Morelhão[a,*], G.E.S. Brito[a], E. Abramof[b]

[a]*Instituto de Física, USP, CP 66318, 05315-970 São Paulo, SP, Brazil*

[b]*Instituto Nacional de Pesquisas Espaciais, LAS, CP 515, 12141-970 São José dos Campos, SP, Brazil*

Abstract

Recently, a significant amount of studies have been carried out on sol–gel films for optical applications, mostly motivated by the quickness and low cost of the film preparation process. Overcoating films of different density and thickness can produce waveguides for visible light as well as for X-rays. In order to preserve the coherence properties of the guided light, improvements in the current quality of the films are necessary as well as an appropriated technique for structural characterization and quality control. X-ray specular reflectivity can be such a technique, but it is limited by the complexity of the internal nanostrutucture of the films. In this work, we have developed a procedure to fit the specular reflectivity and extract the exact density profile of sol–gel films. It is applied to analyze a single compound film produced from a sol–gel of Er_2O_3 nanoparticles. It correlates the density variations and roughness with the steps of the preparation process. Moreover, we have also characterized an X-ray waveguide of $Er_2O_3/TiO_2/Er_2O_3$ and theoretically optimized its structure to demonstrate the effects of density floating and roughness on the waveguidance efficiency.

Keywords: Sol–gel films; X-ray reflectivity; Data fitting; Genetic algorithm; X-ray waveguide

1. Introduction

Sol–gel films have been widely investigated for optical applications due to their very low cost and fast preparation process [1,2]. Layered films of different density and thickness can easily produce waveguides for visible light [3–7] as well as for hard X-rays [8]. In high-brilliance synchrotron radiation sources, X-ray waveguides have become an important optical device that can lead to new developments in X-ray microscopy [9] and in characterization techniques with submicro-scale resolution [10]. Waveguides are basically a film composed of a light material onto a heavier one, whose waveguidance efficiency is strongly enhanced by overcoating the film with a very thin layer as dense as the bottom one. For most applications, coherence of the guided X-rays is crucial. Interface roughness does generate incoherent scattering that compromises the coherence of the beam exiting the waveguide and, at values above a few nanometers, the roughness can destroy the waveguidance.

The detailed structure of sol–gel films, i.e. films prepared by coating from a sol–gel solution, is still under investigation [11]. The dynamics of nanoparticles coalescence during firing, or heat treatment, can generate abrupt density variations and porosity inside a single film. Both features contribute to reduce the lateral coherence length and give rise to a sort of internal roughness that, in terms of incoherent scattering, is exactly the same as interface roughness. Then, at the present status of film preparation, it is evident that a characterization tool is needed for analyzing the structure of the films in a nanometer scale. It would provide the necessary information to improve the procedures for producing high quality sol–gel films. Density profile and internal roughness, besides thickness, are the most important parameters to be extracted and correlated to the variables of the preparation procedure, such as coating speed and firing temperature.

X-ray specular reflectivity is a non-destructive characterization method applied to a large variety of thin film materials. For laterally uniform films, grazing incidence reflectivity measurements can be applied equally effectively to single crystal, polycrystalline or amorphous films. The specular scattering in the region just above the critical angle contains information not only on the longitudinal

*Corresponding author. Tel.: +55-11-3091-7012; fax: +55-11-3091-6706.

E-mail address: morelhao@if.usp.br (S.L. Morelhão).

0925-8388/02/$ – see front matter
PII: S0925-8388(02)00342-0

electron density and thickness of sub-micron films, but also surface and interface roughness on the atomic scale. Since a simple inverse transformation of the scattered intensity to obtain all the film parameters is not possible, the adopted approach for the interpretation of reflectivity data has been the simulation of the scattering from a model structure and adjustment of parameters until a good fit is obtained. In spite of all difficulties involved in this last step, i.e. in the adjustment of parameters, the technique is limited by the previous knowledge of the structure of the films. Exceptions are single layers with uniform density and thickness, which are extracted directly from the curves. Otherwise, the best possible fit will be satisfactory only when the correct model has been assumed, the model that has a number of adjustable parameters for which there is a set of values that describe the actual structure of the film. For sol–gel films, the uniform one-layer model is useful only to estimate the thickness and average (or apparent) density [11].

In this article, we describe some adjustable model structures able to extract, from the X-ray specular curve, the longitudinal density profile and roughness of sol–gel films. In the models, the heavy duty of adjusting the parameters, until the reflectivity simulation program [12] generates the best fit for the scattering data, is carried out by the differential evolution algorithm (DEA) [13]. Evolutionary algorithms, one particular class of genetic algorithms, apply some of the known mechanisms of evolution to solve optimization problems. Through simple mutation, recombination and selection schemes, the DEA finds the parameter vectors that yield the smallest value of the error function, where each n-dimensional parameter vector contains a set of values for all n adjustable parameters of the models. Mutation is an operation that makes small random changes in the population of vectors, and it is critical for maintaining the diversity in the population. This scheme allows the DEA to reach the global minimum of the error function instead of getting stuck on a local minimum. However, the accessible space of parameter values is defined by the user's guess at the structure, when the range of allowed values for each adjustable parameter is imposed. Therefore, the global minimum for a given model will always be found by the DEA if it falls into the guessed accessible space, and if this space is narrow enough to allow the evolution to be concluded in a reasonably short period of time.

2. Experimental

A single compound film (Er_2O_3 film) was prepared by three dip-coatings of a glass plate (2.475 ± 0.025 g/cm^3) in a sol–gel of Er_2O_3 nanoparticles. Each dip was followed by firing at 500 °C for a few minutes in order to eliminate the gel and the organic cap of the nanoparticles. The detailed process for producing such sol–gels has been described elsewhere [14]. Using this sol–gel and a second one of TiO_2 particles, produced by the same process, a multilayered film (WG film) was also prepared. It has five layers; the odd layers (1st, 3rd and 5th) were coated by just one dip in the sol–gel of Er_2O_3, and the even layers by two dips in the sol–gel of TiO_2.

The grazing incidence X-ray reflectivity measurements were performed in a high-resolution X-ray diffractometer (Philips X′Pert-MRD) equipped with a Cu X-ray tube in the line focus. The primary optics (for the incident beam) was composed of a Soller slit, a $1/32°$ divergence slit and an attenuator, and for the secondary optics (reflected beam) we used, before the detector, a parallel beam collimator, a 0.1 mm anti-scatter slit and a flat crystal graphite monochromator. Before starting measuring, the sample height and the goniometer zero points ($2\theta=0$ and $\omega=0$) were precisely adjusted. The reflectivity spectra were recorded by a longitudinal scan in the reciprocal space, $\omega/2\theta$ scan. The attenuator is used for angles lower than a pre-defined angle to avoid the detector damage due to a very intense incident radiation. The attenuator factor is automatically computed during the measurement, allowing a dynamical scale of eight orders of magnitude.

3. Results

Fig. 1 shows the experimental reflectivity curves (open circles) of the Er_2O_3 film (a) and the WG film (b). In order to fit the first experimental curve three possible models for the structure of the films were considered at the beginning: the one-layer model, the multi-slab model and the multi-slab model with roughness at the interfaces of each slab (hereafter named MSr). The adjustment of the parameters was carried out by the DEA and the improvement of the fitting is driven by mean-absolute error of the log-transformed data. In the Parratt's recursion-relation formalism [15] employed by the simulation program, the effects of roughness is taken into account by reducing the Fresnel reflection amplitude, r_F, of each interface. The expression for such reduction at the jth interface, between slabs j and $j+1$, is given [16] by $r(j)=r_F(j)\exp[-2(k_{z,j}k_{z,j+1})^{1/2}\sigma_j]$, where σ_j stands for the Gaussian width of the interface due to roughness, and $k_{z,j}$ is the longitudinal component of the wavevector in the slab j. Note that, σ_j also accounts for reduction in the lateral coherence length of the interfaces besides the physical roughness. Then, it is possible to have a value of σ_j larger than the thickness of its respective slab. The attenuation of the X-ray beam is also included in the reflectivity simulation program by means of a complex refractive index of the materials [12].

In the case of the Er_2O_3 film, although the one-layer model as well as the multi-slab model with adjustable density can provide an estimation of the thickness ($\approx$24 nm) and of the average density (6.93 g/cm^3), none of them are able to fit the experimental curve. The remarkably good

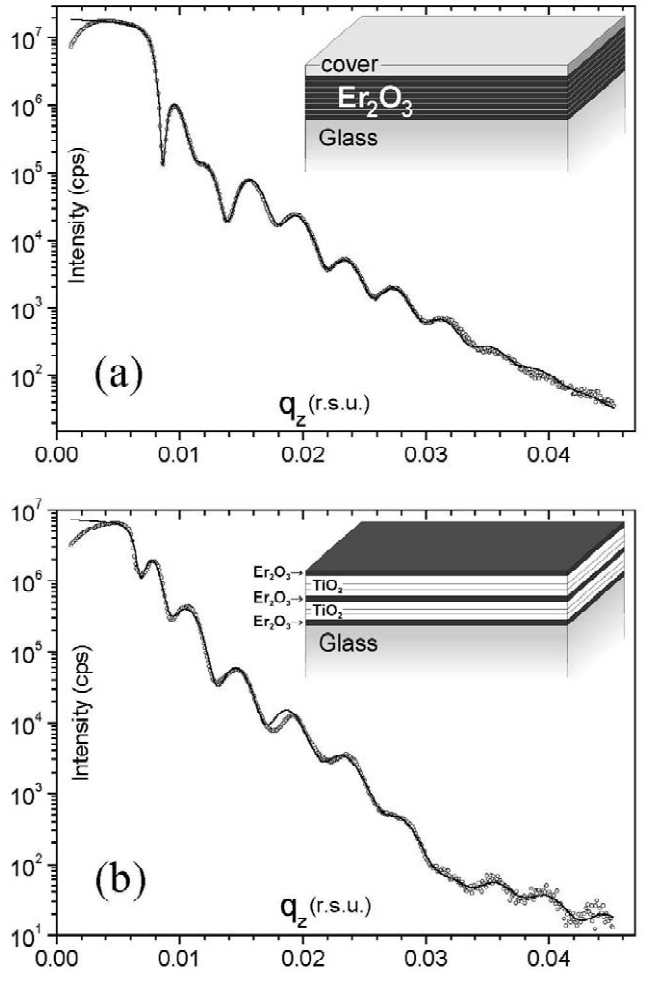

Fig. 1. X-ray specular reflectivity curves from the erbium oxide sol–gel film (a) and the multilayered Er_2O_3/TiO_2 film, the WG film (b). The experimental curves—open circles—are compared to the best fitting curves—straight lines—obtained with the respective MSr models. An illustration of the models are shown in the insets, where the Er_2O_3 film is divided into eight slabs plus a cover layer, and each TiO_2 layer in the WG film was divided into three slabs. The parameter values extracted with these MSr models are given in Fig. 2.

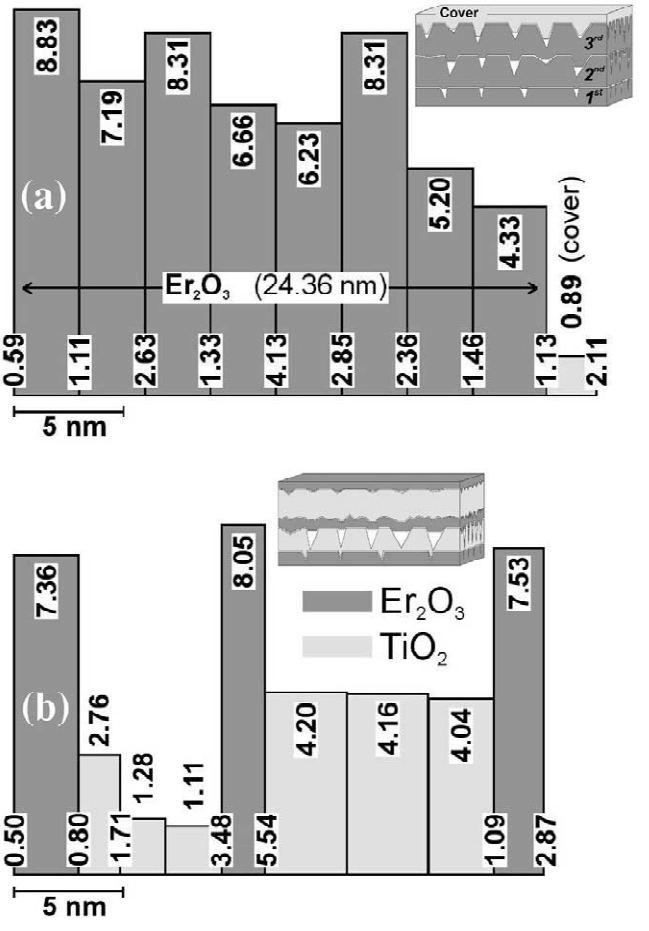

Fig. 2. Model structures for the Er_2O_3 (a) and WG (b) sol–gel films that provide the fitting of the X-ray specular reflectivity curves in Fig. 1. The bars height stands for the density values (in g/cm^3) written at the top, and the number in-between bars are the interface roughness (in nm). The cover layer (2.3 nm) of $H_2O+CO_2+O_2+N_2$ is assumed for the Er_2O_3 film due to possible air contamination. The explanation for the decreasing density gradient observed in the Er_2O_3 film is schematized at the top inset, where the surfaces after the 1st, 2nd and 3rd dip are located around z equal to 6, 15 and 24 nm, respectively. Similar density gradient is also observed in the first TiO_2 layer of the WG film, whose scheme is given at the bottom inset.

fitting shown in Fig. 1a could only be achieved when roughness is allowed at the interfaces of the adjacent slabs. The exact structure of the film determined with this MSr model is shown in Fig. 2a. It was necessary to divide the film thickness into eight slabs, seven slabs of 3 nm plus one top slab of adjustable thickness. A cover layer of 2H:1C:2N:5O, which might be present due to air contamination, have been added to the model, and it has significantly improved the quality of the fitting. Then, for this model there were 21 parameters adjusted by the DEA. With the density values of all slabs limited in the range from 4 to 9 g/cm^3, their best-fit values do not differ from those in the figure by more than 2.5%. In the accessible space defined by this range, the values in the initial parameter vector do affect the evolution time required by the DEA for minimization of the error function. On the other hand, the sensitivity of the fit with the roughness depends on the density difference throughout each interface. The highest and lowest sensitivities are for the roughness at $z=0$ and $z=12$ nm, respectively. Changes of 2% and 32% in the roughness values at these interfaces would produce the same fit deviation of 5%.

For fitting the scattering data from the WG film, we also have to use the MSr model. However, in this case, the thickness of the slabs would have to be adjusted, besides their densities and interface roughness. Then, the DEA had to handle the adjustment of seven more extra parameters—standing for the thickness of the slabs—than in the case of the single compound film. The final MSr model structure responsible for the good fit shown in Fig. 1b is given in Fig. 2b. Each TiO_2 layer was divided into three slabs with a total thickness of 6.62 nm and 10.53 nm for the first and

second layers, respectively. Internal roughness and a density gradient are observed only in the first layer, whose average density is much smaller that the nominal value (4.12 g/cm^3) of the TiO_2 compound. High values of roughness were found at both interfaces of the Er_2O_3 layer at the middle of the structure. The assumption of a cover layer did not improve the fit quality. The small discrepancy of the fit observed around $q_z = 1.8\times10^{-3}$ $Å^{-1}$, might arrive due to some density profile in the Er_2O_3 layers, which could not be satisfactorily resolved by our nine-slab model. Although the DEA never stop the auto fitting, unless required to, 28 adjustable parameters is about the limit of its practical efficiency.

4. Discussions

The most important physical feature in the MSr model is that by introducing roughness at the interfaces of adjacent slabs, the model was able to simulate the effects of the internal roughness present in a single compound layer. Since this internal roughness stands for the reflectivity reduction, it demonstrates that some amount of diffuse scattering is generated inside the film. Otherwise, the multi-slab models without internal roughness would have succeeded in fitting the experimental curve and extracting the longitudinal density profile, which were more complex than just the average density for the Er_2O_3 film. The two minima of the density profile observed in Fig. 2a, around 4.5 and 12 nm, are correlated to the number of dips (three in this case) used to prepare the film. After each dip, the fired layer has a lower density towards the surface, and subsequent overcoating and heating did not restore the density of the previous surface. The first dip seems to provide a near 6 nm thick layer and each subsequent dip has added approximately 9 nm to the total thickness. Then, a length scale resolution of 3 nm—the slab thickness—was necessary to resolve the profile. The presence of the low-density cover layer has been observed in other sol–gel films [11]. And, although its thickness (2.3 ± 0.5 nm)[1] is still larger than the one expected for a contamination layer due to absorption of air species, it should be mentioned that this value was significantly reduced regarding the value (4.8 ± 1.0 nm) estimated by using the one-layer model.

Reliability of the parameters obtained by the evolutionary algorithm, the DEA, is a very complicated issue, as it is in any other X-ray analysis based on curve fitting. It depends fundamentally on one factor: the quality of the final fit. The perfect fit would be the one where the minimum value of the error function is exclusively due to the statistical noise on X-ray generation and detection—calculated by a Poisson distribution. That will be the case when the structure of the sample is accurately described by the model, there are no errors associated with the simulation of the X-ray scattering, and there are no systematic errors present in the experimental data. Materials analysis by X-ray data fitting works assuming that there is only one model able to produce the perfect fit, and when it is obtained, the model responsible for such fit is taken as an accurate description of the sample. The problem, however, resides in the fact that in general there is not a model able to reproduce all features existent in the real samples. Therefore, the best-fit parameter values for a given model may carry some intrinsic errors due to a deficiency in the model, which can not be estimated. For instance, the 50% variation (or error) in the thickness of the cover layer in the Er_2O_3 film extracted by the one-layer model in comparison to the one obtained by the MSr model. When a reasonably good fit is archived, although not the perfect one, we expect that the deficiencies of the model do not significantly affect the best-fit parameter values, at least not to the point where there is change to any physical interpretation of the structure of the sample. In order to be very specific, the MSr models are very efficient for sol–gel films because they allow the necessary degree of freedom for the models to take into account the reduction in the specular reflected intensity by density gradients as well as by diffuse scattering due to internal roughness. Their deficiency is the finite number of slabs used to represent the density profile of the films. In the WG film, several more slabs would be necessary to obtain a really good fit of the experimental data—it is stated because the fit quality improves with the number of slabs in which the two TiO_2 layers have been divided into. However, it will not change the fact that there is an accentuated gradient in the density profile around $z=6$ nm, Fig. 2b, neither the order of magnitude of the thicknesses, or the existence of roughness at the interface of the layers with different composition.

The value of roughness at the final surface of a film can be critical for waveguides of sol–gel films because it will be the interface between two compounds of very different densities. For this reason, the WG film was prepared in order to observe the level of roughness present at the interface of a dense (Er_2O_3) and a lighter (TiO_2) layer, and how it would affect the intensity of the possible guide modes. In the specular reflectivity curve, the guidance of the X-rays are characterized by a strong reduction in the reflectivity at some incidence angles below the critical angle, θ_C, of the dense layer. At these angles, a standing wave is formed inside the structure and the energy flow is parallel to the surface. The first dip observed in the specular curve of the WG film, Fig. 1b, is below θ_C ($\approx1214''$) of the Er_2O_3 film—for the measured density of 7.36 g/cm^3. The simulation program used before is also useful to theoretically explore the effects of the features founded in the WG film that seem to have destroyed the guidance of this mode.

The thickness of the Er_2O_3 layer at the bottom of the

[1]Error estimated by fit deviation bouncing 5%.

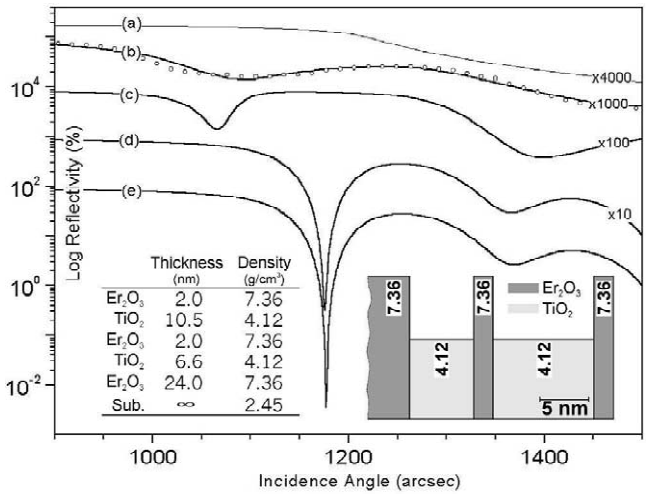

Fig. 3. Theoretical specular reflectivity curves around the critical angle—given by curve (a)—of the Er_2O_3 compound with a density of 7.36 g/cm^3. Curve (b) is the simulated scattering for the WG film structure—Fig. 2b—obtained from fitting the experimental data (open circles). By keeping this exact model, but increasing the thickness of the bottom layer to 24 nm, curve (c) is generated. Curves (d) and (e) shown the effects that the density gradient and the roughness had on the guided mode, respectively. Both insets, the table or the illustrative scheme, specify the idealized structure—without roughness—responsible for curve (e).

WG film was not thick enough to allow a total external reflection. Then, by increasing its thickness to 24 nm—the same thickness of the Er_2O_3 film analyzed here—the occurrence of a guided mode is more evident as can be seen in the curve (c) of Fig. 3, at the incidence angle of 1060″. When the density gradients characterized in the TiO_2 layers are removed in the simulation, and the densities set equal to the nominal value, the guide mode shifts from its previous position to 1180″, curve (d) of Fig. 3. Finally, by making all interfaces and surfaces sharp, we have the idealized structure shown in the insets of Fig. 3, which is responsible for curve (e) in the figure. The reduction in reflectivity at the center of the guide mode—regarding the nearest maximum at right-hand side—are 82.25, 99.90, and 99.99% for curves (c), (d), and (e), respectively. According to these simulations, density gradients in layered sol–gel films is more harmful to the confinement of energy in waveguides than the roughness levels actually observed in such films.

5. Conclusions

We have demonstrated that detailed density profiles of single compound sol–gel films as well as multilayered films can be extracted from X-ray specular reflectivity curves. The calculated spectrum can be precisely adjusted to the measured one by using multi-slab models with internal roughness, i.e. with roughness at each slab interface. It takes into account the diffuse scattering generated inside the film, which is evidence of the presence of porosity. The density profiles extracted by the appropriated models allow us to conclude that the shrinkage during firing introduces some sort of ‘rifts’ at the intradip surfaces, as schematized in the insets of Fig. 2. The decreasing density gradient towards the surface due to the rifts seems to affect more the guided intensity than the internal roughness, which is also a consequence of the rifts.

Acknowledgements

The authors would like to thank the Brazilian funding agencies FAPESP (proc. number 99/00273-8) and CNPq (proc. numbers 301617/95-3). We also thank Dr Keith Bowen and Dr Matthew Wormington as well as the agents of Bede Scientific in Brazil (www.raioxconsultoria.com) for the REFS mercury software.

References

[1] C.J. Brinker, G.W. Scherer, Sol–Gel Science: The Physics and Chemistry of Sol–Gel Processing, Academic Press, New York, 1990;
L.F. Francis, Matter. Manuf. Processes 12 (1997) 963.
[2] P.K. Biswas, D. Kundu, D. Ganguli, J. Mater. Sci. Lett. 6 (1987) 14811.
[3] A. Bahtat, M. Bouazaoui, B. Mahtat, J. Mugnier, Opt. Commun. 111 (1994) 55.
[4] M.A. Fardad, H. Luo, Y. Beregovski, M. Fallahi, Opt. Lett. 24 (1999) 460.
[5] K.M. Chen, A.W. Sparks, H.C. Luan, D.R. Lim, K. Wada, L.C. Kimerling, Appl. Phys. Lett. 75 (1999) 3805.
[6] C. Coutier, M. Audier, J. Flick, R. Rimet, M. Langlet, Thin Solid Films 372 (2000) 177.
[7] H. Rigneault, C. Amra, S. Robert, C. Begon, F. Lamarque, B. Jacquier, P. Moretti, A.M. Jurdyc, A. Belarouci, Opt. Mater. 11 (1999) 167.
[8] S. Lagomarsino, A. Cedola, S. Di Fonzo, W. Jark, G. Soullié, Appl. Phys. Lett. 71 (1997) 2557.
[9] S. Lagomarsino, A. Cedola, S. Di Fonzo, W. Jark, C. Riekel, Notiziario Neutroni e Luce di Sincrotrone 3 (1998) 1.
[10] S. Di Fonzo, W. Jark, S. Lagomarsino, C. Giannini, L. De Caro, A. Cedola, M. Müller, Nature 403 (2000) 638.
[11] A.P. Rizzato, C.V. Santilli, S.H. Pulcinelli, J. Non-Cryst. Solids 247 (1999) 158;
A.P. Rizzato, C.V. Santilli, S.H. Pulcinelli, J. Sol–Gel Sci. Tech. 19 (2000) 811.
[12] M. Wormington, D.K. Bowen, B.K. Tanner, Mat. Res. Soc. Symp. Proc. 238 (1992) 119.
[13] M. Wormington, C. Panaccione, K.M. Matney, D.K. Bowen, Philos. Trans. R. Soc. Lond. A 357 (1999) 2827.
[14] G.E.S. Brito, C.V. Santilli, S.H. Pulcinelli, A.F. Craievich, J. Non-Cryst. Solids 217 (1997) 41.
[15] L.G. Parratt, Phys. Rev. 95 (1954) 359.
[16] L. Névot, P. Croce, Rev. Phys. Appl. 15 (1980) 761.